

# Efficiency loss breakdown for synchronous rectification scheme for automotive applications

eISSN 2051-3305  
Received on 26th June 2018  
Accepted on 30th July 2018  
E-First on 14th May 2019  
doi: 10.1049/joe.2018.8241  
www.ietdl.org

Dimitrios Sarafianos<sup>1</sup>, Danilo X. Llano<sup>2</sup> ✉, Richard McMahon<sup>2</sup>, Timothy Flack<sup>1</sup>, Stephen Pickering<sup>3</sup>

<sup>1</sup>Electrical Engineering Division, University of Cambridge, Cambridge, CB3 0FA, UK

<sup>2</sup>WMG, University of Warwick, Coventry, CV4 7AL, UK

<sup>3</sup>JaguarLandRover Ltd, UK

✉ E-mail: danilo.llano@gmail.com

**Abstract:** This article presents a synchronous rectification scheme using a six-phase Lundell alternator and a bespoke MOSFET-based active rectifier. The control of the alternator-rectifier system is divided into the hysteresis DC-link voltage control and the switching pattern algorithm. The first allows to keep the DC-link voltage at the required 14V level, while the latter reproduces the same switching pattern as that of a passive rectifier. The system is tested at three different speeds and the results are compared against the body diodes of the MOSFETs in the active rectifier. The harmonic analysis of the generated waveforms indicates the capability of the control algorithm to generate the same switching pattern of a passive rectifier. Finally, the efficiency measurements illustrate a significant efficiency improvement using a synchronous rectification scheme and MOSFETs with low on-resistance.

## 1 Introduction

The electrical power system in a passenger vehicle with an internal combustion engine (ICE) has four main elements: a Lundell alternator for mechanical to electrical power conversion, a rectifier for AC-to-DC conversion, a battery for energy storage and engine cranking and DC loads. The DC-link is nominally set at 14 V to comply with automotive standards. This low voltage creates challenges as modern vehicles require more than 1.5 kW at full load, a current of more than 100 A. This high current leads to significant losses, particularly in the rectification stage.

A conventional vehicle's ICE crankshaft varies typically between 800 and 3000 rpm for idle and cruising speed, respectively. The crankshaft pulley to alternator pulley ratio is around 2.2, thus the alternator's speed varies from 1800 to 6500 rpm. In the present paper, all the given speeds refer to the alternator's speed. This particular speed range is important as the alternator cannot deliver its rated power; therefore, any improvement in the rectifier/alternator system has a significant impact in the power capability [1]. Further to this, the idle to cruise speed range is representative of typical urban driving cycles.

PN junction Zener diode rectifiers have been traditionally used in the automotive industry due to their overvoltage clamping capability. Alternative devices such as Schottky diodes give some increase in the rectifier efficiency [1], but the introduction of a MOSFET-based rectifier using a synchronous rectification switching pattern will be shown to increase the efficiency of the rectifier system significantly. The improvement arises from the fact that the on-state voltage drop across the MOSFETs is much lower than the forward voltage drop of the diode.

Synchronous rectification has been previously studied [2, 3], and there are also products commercially available. To date, the literature has been focused on the comparison between synchronous and passive rectification in terms of overall efficiency, but no details are given about the loss breakdown. In [4], the authors proposed a cost-effective method for introducing a MOSFET three-phase full-bridge synchronous rectifier using a phase angle (of the alternator phase voltage) control scheme to maximise the output power of the alternator. The results indicated that the available power at idle speed was increased by 43% [4]. Their work was extended above idle speed, in [3] up to 6000 rpm, by introducing a stator winding reconfiguration. A comparison

between passive and synchronous rectification from 1250 up to 6000 rpm was made, indicating that at 6000 rpm both schemes have the same output power capability [3]. The authors used switches placed at the DC side to reconfigure the stator windings when the alternator speed reaches 3000 rpm [3].

In [5], a MOSFET gate driver together with a synchronous rectification scheme are introduced, resulting in the efficiency improvement of the system. It is stated that the improvement is more significant at the low speed end, allowing a further decrease of the zero-ampere speed. Efficiency improvement is important in the speed range up to 15,000 rpm [5], compared to the power generation, which becomes similar to that of a passive rectifier above 6000 rpm, according to [3].

An alternator unit has been released by Bosch GmbH using a synchronous rectifier scheme [6]. The patent [7] highlights the use of an active MOSFET-bridge rectifier working in synchronous mode for alternators featuring different stator winding structures: three, five, and seven phases. The efficiency improvements in the Bosch unit are quantified through carbon dioxide emission savings [6]. However, only overall efficiency figures and the extension of the operation region of the alternator to low speeds have been presented in the literature on the topic to date, no details are given on the loss breakdown.

This present paper introduces a synchronisation algorithm that implements a switching pattern resulting in generating the same AC waveforms as those found in a passive rectifier. In addition, a loss breakdown is conducted together with an analysis of the harmonic content of the generated voltage and current waveforms to provide insight into the performance of the proposed system at its different parts. The advantage of the synchronous rectification scheme is due to the low-voltage drop across the MOSFET, owing to its very low  $R_{DSon}$  resistance, but without the complex control scheme and requirements associated with a fully active rectifier. The synchronous rectification scheme considered requires only one voltage sensor and a speed sensor to achieve line synchronisation. No current sensors are necessary for its control. Further to that, the DC-link controller design and tuning is simple, by means of a hysteresis controller in this case.

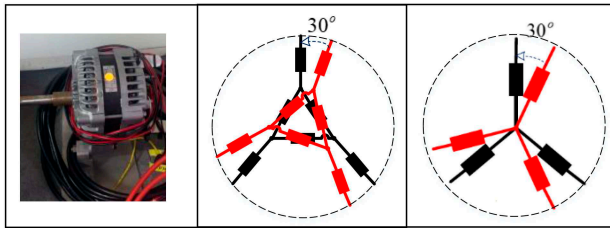


**Fig. 1** Winding construction. Left: Denso Lundell alternator. Centre: Physical construction winding. Right: Equivalent winding configuration

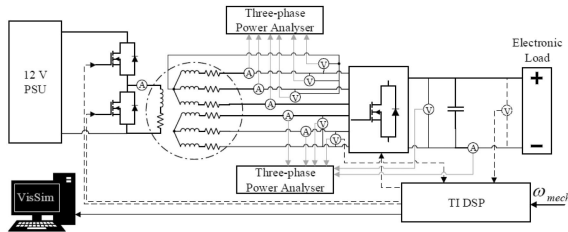


**Fig. 2** Experimental set-up of the synchronous rectifier

## 2 System overview

The Denso SC4 180 A is a six-phase Lundell alternator (Fig. 1 left), consisting of two equivalent balanced windings with an internal delta connection as shown in Fig. 1 (centre). An equivalent impedance was calculated so that the windings can be treated as independent star-connected windings with  $30^\circ$  phase shift between them (Fig. 1 right).

Two identical three-phase rectifiers were designed, built, and tested for this six-phase system using IPP120N08S4-03 MOSFETs. The control scheme was implemented in a TI control board using VisSim software. A PPA5530 power analyser was connected to one of the three-phase windings through calibrated external current shunts and voltage probes. A second identical power analyser monitored the DC-link voltage and current, as well as the other three-phase system using the two-watt meters method. A 20 mF capacitor was connected to reduce the DC voltage ripple and replicate the large capacitance of a battery. Fig. 2 presents the experimental set-up of the synchronous rectifier tests.

### 2.1 Test rig connections

The line current is measured with current shunts (rated at 200 A), placed between the alternator output and rectifier PCB (Fig. 2). The test setup consists of a number of connectors and 16 mm<sup>2</sup> tri-rated cables to handle the high current values. The resistance of the cables and connectors was measured with a four-wire terminal ohmmeter and the mean value was 3.5 m $\Omega$ . This unavoidable parasitic resistance value is significant, considering that is of the same magnitude than the on-resistance ( $R_{DSon} = 2.8$  m $\Omega$ ) of the MOSFET used in the rectifier. Any increase in the series resistance compromises the power capability of the alternator by acting as an extra output impedance and introducing additional conduction losses.

## 3 Active rectifier, DC-link controller, and synchronisation algorithm

### 3.1 Mosfet-based rectifier

The implementation of the synchronous rectification scheme required the use of two three-phase MOSFET active rectifier bridges connected in parallel. The selection of the semiconductor switch for the active rectifier topology was imposed by the application characteristics. With a DC bus voltage of 14 V, currents above 100 A together with the need to minimise conduction losses lead to the use of MOSFET switches. The INFINEON IPP120N08S4-03 MOSFET with the TO220 package was used. This device is of the OptiMOS family, automotive certified, with an on-state resistance of 2.8 m $\Omega$ , as well as very fast turn-on and

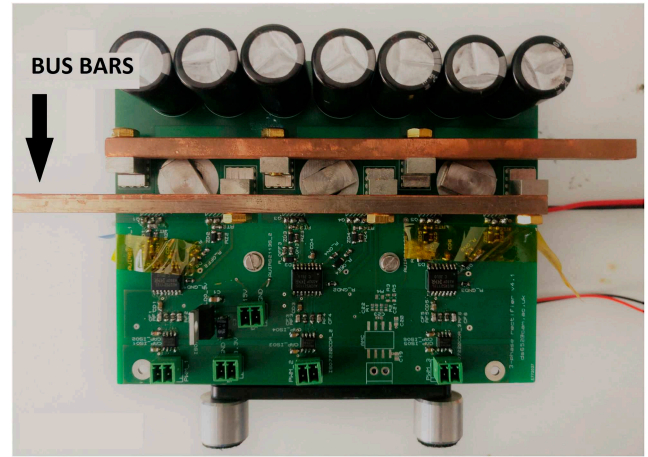


**Fig. 3** MOSFET based rectifier

turn-off times of tens of nanoseconds. Fig. 3 shows the PCB of the three-phase rectifier designed for the high current, low-voltage DC bus in this application.

### 3.2 Body diodes vs. automotive PN junction zener diodes

The study presented here compares a synchronous rectifier with a passive rectifier. The latter uses the body diodes of the MOSFET-based rectifier designed for the synchronous rectification scheme. The reason for this is to keep as far as possible the same test conditions between the two approaches. As already stated in Section 2.1, the parasitic resistance is of the same order of magnitude than the MOSFET on-resistance; therefore, any change in the test rig connections might lead to a noticeable change in the testing conditions. Also, Sarafianos *et al.* have shown in [1, 8] that the efficiency of typical automotive PN junction Zener diodes is lower than other diode technologies, including the body diodes in automotive certified MOSFETs. Therefore, the comparison in this study is still valid if PN junction Zener diodes are considered.

### 3.3 DC-link controller

A hysteresis controller regulates the DC-link voltage to 14 V by adjusting the field current via the duty cycle in a DC chopper. The hysteresis controller operation can be summarised as follows: the DC bus voltage is monitored with a sensor and values fed into the control card. Then, the hysteresis controller regulates the DC-link voltage by controlling the field current by varying the duty cycle of the DC chopper [1].

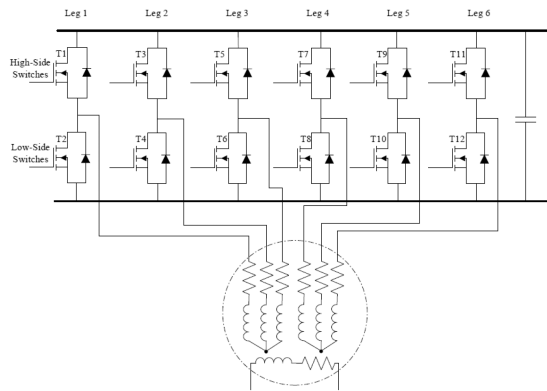
Initially, the required DC voltage is defined as  $V_{dc}$ . Then, a dead-band voltage is defined as  $V_{db}$ , which results in the generation of two reference voltage levels,  $V_{max} = V_{dc} + V_{db}$  and  $V_{min} = V_{dc} - V_{db}$ . The average DC-link voltage is set within the predefined dead-band. In this way, two voltage values are generated,  $V_{max}$  and  $V_{min}$ , defining the DC-link voltage ripple. When the DC-link voltage sensor senses a voltage higher than  $V_{max}$ , then the DC chopper switches off. If the voltage level is lower than  $V_{min}$  the DC chopper switches on. The dead-band and sampling time of the controller are selected to match the dynamics associated with the  $RL$  time constant of the field winding and the acceptable ripple in the DC voltage.

### 3.4 Synchronisation algorithm

The synchronisation algorithm was achieved by sensing the line voltage of the alternator in conjunction with a quadrature encoder. The voltage sensor tracks the zero-crossing of the line voltage. Once the zero-crossing (defined as negative to positive) is identified, an integrator (divided by  $2\pi$  for normalisation to 1) is started adding the speed measurement from the encoder, multiplied by the sampling time. This ramp is compared to the values in Table 1 until the next zero-crossing is detected. Then, the integrator is restarted. The positive to negative zero-crossing point is ignored.

**Table 1** Switching pattern of the synchronous rectifier

1st 3-ph system	Switching condition in VisSim	Conduction path	2nd 3-ph system
T1 ON / T2 OFF	Ramp > 1/6 & < 1/2 (60°–180°)	1,4 / 60°–120°	T7 ON / T8 OFF
T1 OFF / T2 ON	Ramp > 2/3 & < 1 (240°–360°)	6,1 / 120°–180°	T7 OFF / T8 ON
T3 ON / T4 OFF	Ramp > 1/2 & < 5/6 (180°–300°)	3,6 / 180°–240°	T9 ON / T10 OFF
T3 OFF / T4 ON	Ramp > 0 & < 1/3 (0°–120°)	2,3 / 240°–300°	T9 OFF / T10 ON
T5 ON / T6 OFF	Ramp > 5/6    < 1/6 (300°–60°)	5,2 / 300°–360°	T11 ON / T12 OFF
T5 OFF / T6 ON	Ramp > 1/3 & < 2/3 (120°–240°)	4,5 / 360°–60°	T11 OFF / T12 ON

**Fig. 4** Schematic of the alternator connections to the two-parallel active rectifier circuits

The angle values in Table 1 are established to mimic the switching pattern of an uncontrolled rectifier and are normalised to one for easier implementation.

This pattern was later implemented in the MOSFET-based rectifier, working as a synchronous rectifier, in Fig. 4.

The synchronisation algorithm was tested in MATLAB-Simulink with the Simscape Power Systems toolbox. The algorithm was initially tested using an ideal six-phase power supply but it was also tested with the rectifier and the model of the Lundell generator developed in [1] including the harmonics induced in the line voltage due to the non-linear load. Fig. 5 shows the results in both cases.

#### 4 Efficiency and harmonics analysis

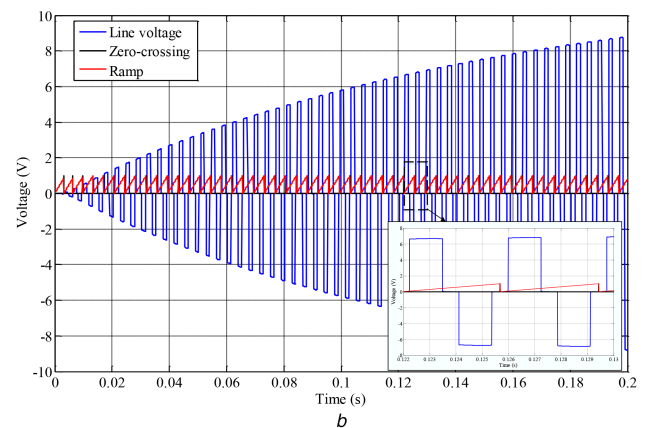
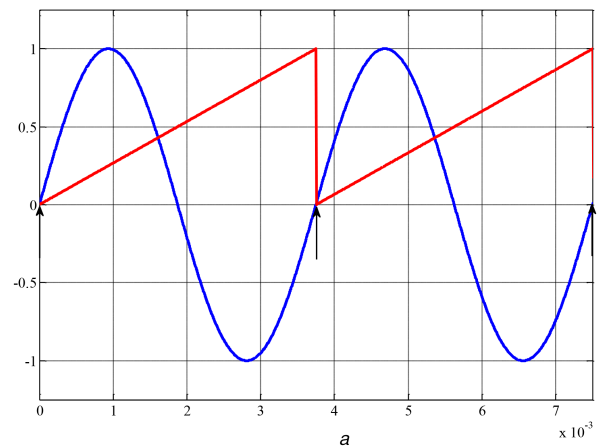
The temperature of the alternator stator winding was monitored until an equilibrium of 23°C was reached. It is recognised that there will be a wide range of operating temperatures, but a fixed temperature was used for simplicity in the lab. In this way, the stator winding resistance was the same for every rectifier experiment. Each rectifier was tested at 14 ± 0.1 V DC output voltage for 500 and 1 kW of DC output power. The alternator speed points were 2000, 4000, and 6000 rpm representing idle to cruise speeds of a conventional ICE vehicle. At every test condition point, the input torque, the alternator speed, the alternator's output power, the AC line rms current, the DC output voltage and DC current values were captured.

##### 4.1 Efficiency

The performance of the synchronous rectification scheme was compared against that of the rectifier using the MOSFET body diodes. Fig. 6 presents the power breakdown and rectifier efficiency of the two schemes for different speeds at 1 kW of output power. The breakdown of losses is done using the procedure described in [1, 8]. The rectifier efficiency is defined by the following equation:

$$\eta_{\text{rectifier}} = \frac{P_{\text{dc}}}{P_{\text{ac}}} \quad (1)$$

It is evident from the experimental results that the synchronous rectifier offers a significant efficiency improvement compared to passive rectification. The rectifier losses of the synchronous

**Fig. 5** Synchronisation algorithm- simulation

rectification scheme, compared to the conventional passive rectifier, are decreased from 152 to 32 for the 1 kW, 2000 rpm measurement point, which in turn is almost 75% reduction in losses at the rectification stage. Fig. 6 also shows that the passive rectifier losses are the highest in the system. At 2000 rpm, the passive rectifier losses are 1.2 times higher than the stator copper losses, and almost five times higher than friction and windage losses. On the other, the losses in the synchronous rectifier are the lowest in the electric system. As an example, at 2000 rpm, the synchronous rectification losses are the same as the friction and windage losses (32 W) and almost four times lower than the stator copper losses. The ratio between passive and synchronous rectification losses is almost constant throughout the entire speed range, but the rectifier losses have a lower percentage of the overall system losses when the speed increases due to higher machine related losses: iron and friction and windage losses, therefore, any improvement in rectification efficiency will have more impact at low speeds.

##### 4.2 Harmonic analysis

To verify that the synchronous rectifier generates the same waveforms as a passive rectifier, the generated AC waveforms were captured. Figs. 7a and b present the voltage and current waveforms of both schemes at an operating point of: 2000rpm, 500 W output power, and 14 V DC voltage. The harmonic

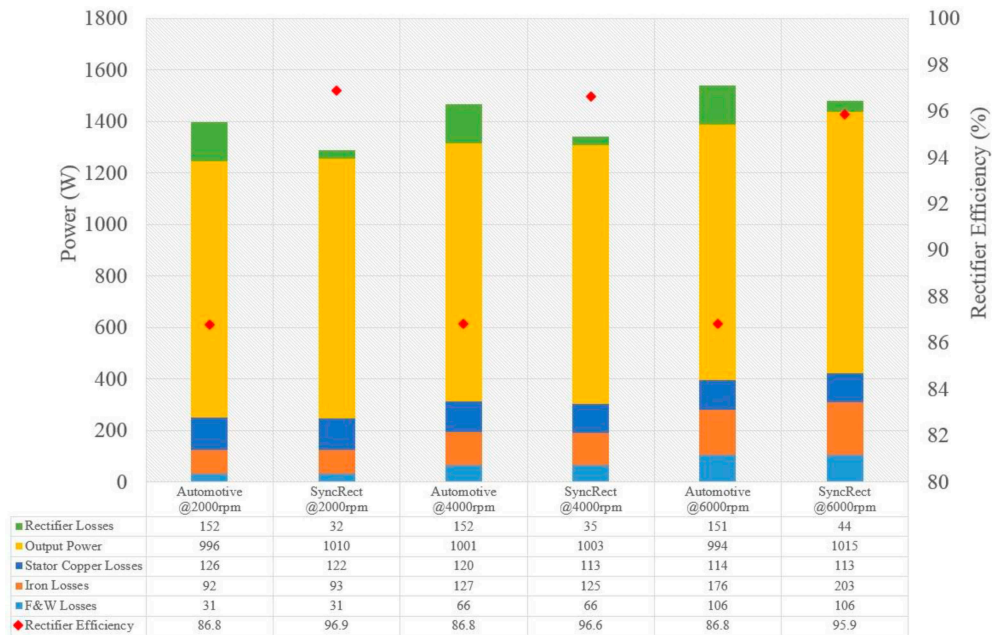


Fig. 6 Loss breakdown for synchronous and passive rectification at different speed points for 1 kW of output power

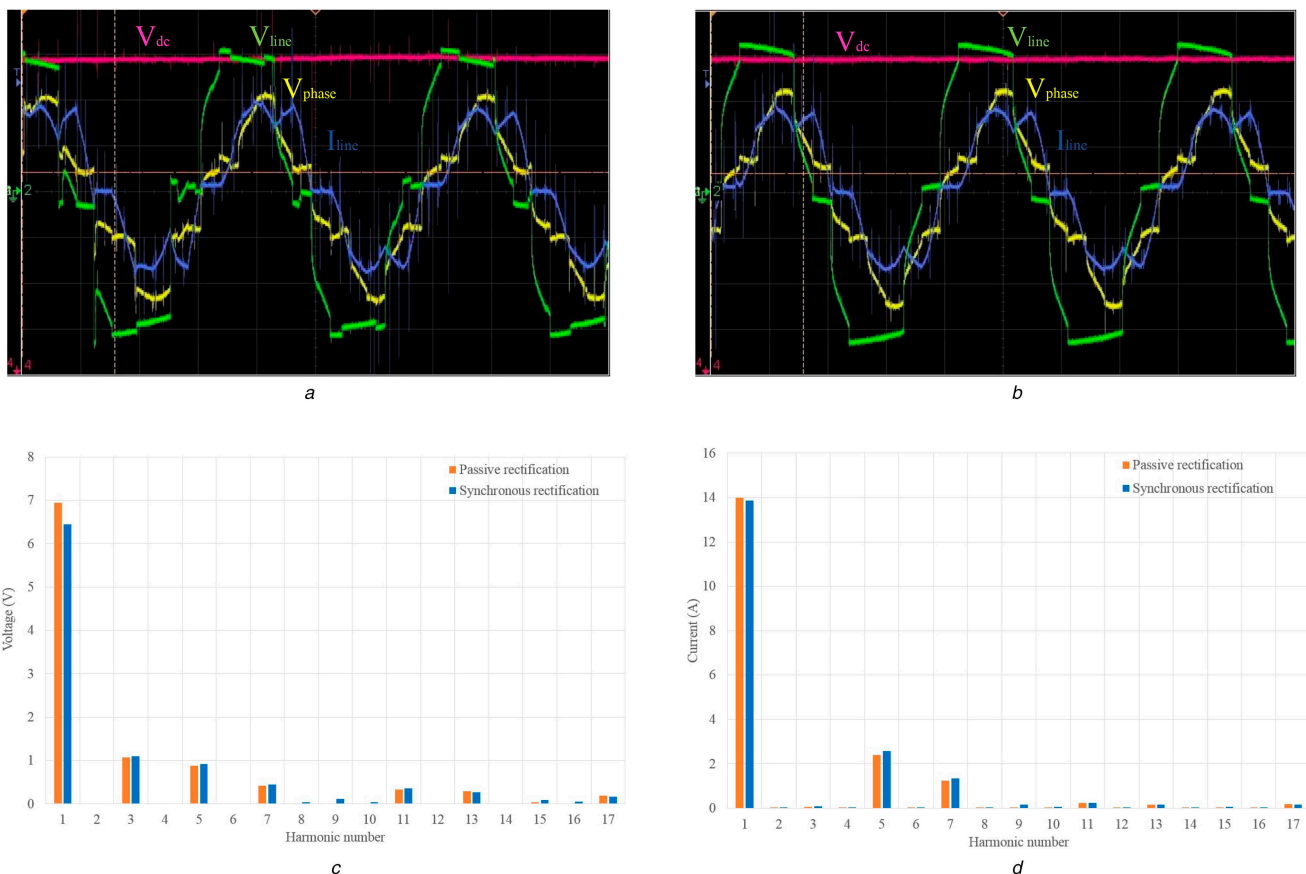


Fig. 7 Voltage and current waveforms and harmonic analysis of the passive and synchronous rectification

distortion of the line voltage and current waveforms of the synchronous rectifier are almost the same as those of the passive rectifier. A harmonic analysis of the line voltage and current waveforms was performed for the same operating point resulting in Figs. 7c and d. The fundamental component of the current is almost the same for both rectification schemes but the fundamental component of the AC voltage at the input to the passive rectifier is considerably higher. This was expected and is due to the forward voltage drop of the diode component, while the MOSFET's forward voltage drop is expected to be much lower because of the very low on-resistance (2.8 mΩ) of the MOSFETs used [9].

The voltage waveform includes multiple harmonic components, being the third, fifth, and seventh main ones. However, the current does not include a third harmonic indicating that this harmonic does not contribute losses to the alternator. This was expected as the alternator does not have a neutral point (Section 2). Space harmonics are produced by the stator mmf under loaded conditions with the most significant being the fifth and seventh [9]. All the high-order harmonics of both, voltage and current waveforms, are <5% different. The power that the harmonics contribute to the losses for both schemes are very low compared to the fundamental components.

**Table 2** Estimated conduction losses per device at different junction temperature

Temperature	25°C		175°C	
passive rectifier				
$I_{rms}$ [A]	50	100	50	100
$V_f$ [V]	0.82	0.90	0.62	0.74
$P_{passive}$ [W]	41	90	31	74
synchronous rectifier				
$I_{rms}$ [A]	50	100	50	100
$R_{DSon}$ [mΩ]	2.2	2.2	3.7	3.7
$P_{sync}$ [W]	5.5	22	9.5	37
comparison of losses				
$P_{sync}/P_{passive}$ [%]	13.8	24.4	30.6	50

### 4.3 Operation at higher temperature

The loss breakdown presented in Fig. 6 shows that the main difference in losses between the synchronous and passive rectifier occurs at the rectification stage, comprising conduction, and switching losses. The switching losses in the synchronous rectifier can be neglected as even in a fully active rectifier they only comprise a minimal part of the total losses in low-voltage, high current applications [1, 10]. The conduction losses per device can be roughly estimated using (2) and (3) for the passive and synchronous rectification, respectively.

$$P_{passive} = I_{rms} V_f \quad (2)$$

$$P_{sync} = I_{rms}^2 R_{DSon} \quad (3)$$

where  $I_{rms}$  is the current across the device,  $V_f$  is the forward voltage of the MOSFET body diode, and  $R_{DSon}$  is the on-resistance of the MOSFET.

The parameters are extracted from the respective curves available in the manufacturer's datasheet. Two junction temperatures are considered: 25°C and 175°C (maximum junction temperature).

Table 2 shows that even at critical working conditions, 175°C and 100 Arms per device, the conduction losses in the synchronous rectification are no more than 50% of the losses in a passive rectifier operating at the same conditions.

## 5 Conclusions and future work

The work here shows how increased efficiency is obtained with a synchronous rectification scheme compared to the passive rectifier using the MOSFET body diodes. More than 100 W (from 152 to 44 W) were saved at 1 kW output power. Even at the maximum temperature, the synchronous rectifier will have around 50% less losses than the passive rectifier. This substantial efficiency improvement (10% saving), owing to the very low on-resistance, allows the alternator to produce more power at its low-speed range, where typically its power capability is decreased. The results shown here can be extended to automotive PN junction Zener diodes as well.

The synchronous rectification scheme presented here does not require advanced synchronisation and control algorithms. It can be achieved by means of a voltage sensor and speed sensor. The DC link is regulated with a hysteresis controller. This is advantageous compared to a fully active rectifier where current sensors, a precise position encoder, and advanced control loops are necessary.

The active rectifier was designed with standard automotive MOSFETs, appropriately rated for the current requirements, in TO-220 packaging. It was estimated that even at critical operating conditions, 175°C (junction temperature) and 100 A per device, the losses of the synchronous rectifier would be 50% lower compared

to a passive rectifier. Further reductions are expected if surface-mounted devices with special packages are used. For example, a MOSFET with a similar rating to the one here, but in the TO-Leadless package, has 1.2 mΩ on-resistance, which is around 50% lower than the devices employed in this study.

Synchronous rectification is more efficient than passive rectification throughout the entire speed range of the alternator, but the most significant gain is seen at the low-speed end (idle to cruise speed), where the rectification losses have a higher percentage of the overall system losses. This range is particularly important as the power capability of the alternator reduces at low speeds, making any efficiency improvement more attractive. Additionally, regular urban driving cycles are within this speed range, which would be translated in an advantageous gain during the most likely driving conditions.

In the future, the authors intend to include work in a sensorless speed estimator to replace the quadrature encoder. In addition, different rectification strategies will be explored to evaluate their impact on the overall system efficiency.

## 6 Acknowledgment

This research was supported by Jaguar Land Rover Ltd.

## 7 References

- [1] Sarafianos, D.: 'Lundell alternator modelling and efficiency improvement of conventional vehicle electrical power systems'. Ph.D. dissertation, 2016
- [2] O'Gorman, T., Stephens, D., Bohn, T., *et al.*: 'Automotive alternator synchronous rectification via self-sensing method for improved vehicle fuel consumption'. 2007 IEEE Industry Applications Annual Meeting, New Orleans, USA, September 2007, pp. 1726–1730
- [3] Liang, F., Miller, J.M., Xu, X.: 'A vehicle electric power generation system with improved output power and efficiency', *IEEE Trans. Ind. Appl.*, 1999, **35**, (6), pp. 1341–1346
- [4] Liang, F., Miller, J., Zarei, S.: 'A control scheme to maximize output power of a synchronous alternator in a vehicle electrical power generation system'. Industry Applications Conf., 1996. Thirty- First IAS Annual Meeting, IAS '96, Conf. Record of the 1996 IEEE, San Diego, USA, October 1996, vol. 2, pp. 830–835
- [5] Rees, S., Ammann, U.: 'A smart synchronous rectifier for 12 v automobile alternators'. 2003 IEEE 34th Annual Power Electronics Specialist Conf., 2003 (PESC '03), Acapulco, Mexico, June 2003, vol. 4, pp. 1516–1521
- [6] Gmbh, R.B.: 'Bosch eco-innovations: fine-tuning for the co2 fleet target'. bosch-presse.de, Techreport, 2015
- [7] Wolf, G., Mehringer, P., Reutlinger, K., *et al.*: 'Activation of a synchronous rectifier', US Patent 9,203,327, 1 December 2015. Available at <http://www.google.ch/patents/US9203327>
- [8] Sarafianos, D., Logan, T.G., McMahon, R.A., *et al.*: 'Alternator loss breakdown and use of alternative rectifier diodes for improvement of vehicle electrical power system efficiency'. 2014 16th Int. Power Electronics and Motion Control Conf. and Exposition, Antalya, Turkey, September 2014, pp. 502–507
- [9] Boldea, I.: *The electric generators handbook, variable speed generators* (CRC Press/Taylor & Francis, London, 2005)
- [10] Sarafianos, D., Llano, D.X., McMahon, R.A., *et al.*: 'Efficiency improvement and power loss breakdown for a lundell-alternator/active-rectifier system in automotive application'. 2017 43rd Annual Conf. of the IEEE Industrial Electronics Society, Beijing, China, November 2017